

Long-Period Seafloor Seismology and Deformation under Ocean Waves

by Spahr C. Webb and Wayne C. Crawford

Abstract The deformation of the seafloor under loading by long-period ocean waves raises vertical component noise levels at the deep seafloor by 20 to 30 dB above noise levels at good continental sites in the band from 0.001 to 0.04 Hz. This noise substantially limits the detection threshold and signal-to-noise ratio for long-period phases of earthquakes observed by seafloor seismometers. Borehole installation significantly improves the signal-to-noise ratio only if the sensor is installed at more than 1 km below the seafloor because the deformation signal decays slowly with depth. However, the vertical-component deformation signal can be predicted and suppressed using seafloor measurements of pressure fluctuations observed by differential pressure gauges. The pressure observations of ocean waves are combined with measurements of the transfer function between vertical acceleration and pressure to predict the vertical component deformation signal. Subtracting the predicted deformation signal from pressure observations can reduce vertical component noise levels near 0.01 Hz by more than 25 dB, significantly improving signal-to-noise ratios for long-period phases. There is also a horizontal-component deformation signal but it is smaller than the vertical-component signal and only significant in shallow water (<1-km deep). The amplitude of the deformation signal depends both on the long-period ocean-wave spectrum and the elastic-wave velocities in the oceanic crust. It is largest at sedimented sites and in shallow water.

Introduction

Broadband seismic observations are becoming routine on the deep seafloor. The first permanent seismic observatory (H2O) was installed on a seafloor cable between Hawaii and California in 1998 (Chave *et al.*, 1998). However, long-period seismic sensors at or under the seafloor record not only earthquake arrivals but also the ground deformation under long-period ocean-wave loading. These waves, known as infragravity waves, produce significant seafloor pressure fluctuations at periods of 30 sec and longer (<0.03 Hz). At still longer periods, seismic sensors detect the deformation due to the loading of the ocean tides and tide of the Earth. The ocean tidal loading problem has been extensively studied using observations from land sites (Lambert, 1970; Farrell, 1972; Agnew *et al.*, 1995), but the effect of infragravity waves on seismic observations at the seafloor has only recently been recognized. Infragravity waves raise the vertical-acceleration noise levels at a deep seafloor site by more than 10 dB at 0.03 Hz (30s) and more than 25 dB at 0.01 Hz (100s) compared to the nearby station Kipapa on the island of Hawaii (Webb, 1998). The deformation under wave loading dominates vertical-component seismic noise levels at all periods between 0.002 Hz and 0.03 Hz everywhere on the deep Pacific seafloor.

The deformation signal due to infragravity waves is predictable (Crawford *et al.*, 1991). It depends on the amplitude

of the ocean waves, the water depth, and the elastic structure of the oceanic crust and upper mantle. The predictability of the vertical-component deformation signal allows it to be removed from seismometer records using ocean wave measurements from seafloor pressure gauges combined with measurements of the transfer function between pressure and vertical acceleration. The smaller horizontal deformation component is more difficult to remove because it requires measurements of the directional spectrum of infragravity waves.

Infragravity Waves: Sources and Climate

Infragravity waves are ubiquitous throughout the world's oceans, although there are some differences in average spectral levels, particularly between the North Atlantic and Pacific oceans. The term "infragravity wave" describes ocean waves with periods of 25 sec and more (<0.04 Hz); waves longer than the usual wind-driven ocean waves or swell. These waves are not directly driven by wind but instead are generated in shallow water through nonlinear mechanisms from short-period (1–20 sec) ocean waves (Webb *et al.*, 1991; Herbers *et al.*, 1995; Webb, 1998). Most of the long-period-wave energy is trapped near the shoreline as edge waves. Wave-phase velocities increase with water

depth and hence with distance offshore ($c \approx \sqrt{gh}$), so most wave energy traveling offshore is refracted back toward shore. Edge waves are an important source of long-period noise for near-coastal seismic stations (Haubrich, 1970; Agnew and Berger, 1978).

A small portion of the long-period energy leaks off the shelf and propagates in deep water as free surface-gravity waves (Webb *et al.*, 1991; Okihira *et al.*, 1992). Infragravity waves propagate essentially without attenuation across ocean basins in deep water, and each ocean basin is filled with infragravity waves generated by short-period waves that break along its coastlines. The long-period seismic background in an ocean basin is controlled by the infragravity wave climate in that basin, which in turn is determined by the short-period ocean-wave climate driven by winds over the basin.

The Pacific ocean infragravity-wave climate is temporally and spatially stable. There are always strong sources of ocean waves with frequent storms in the high latitudes of both hemispheres and with tropical depressions near the equator. These storms combine to generate energetic ocean waves that reach at least some part of the Pacific coastline at all times. These short-period waves are then sources for infragravity waves throughout the Pacific basin. In contrast, in the smaller North Atlantic basin, there are intervals when there may be no storms at all, during which infragravity-wave amplitudes become very low. The North Atlantic is always less energetic than the Pacific and infragravity-wave energy varies from day to day by more than 30 dB (Webb *et al.*, 1991).

The infragravity-wave climates of the South Atlantic and Indian Oceans are probably more energetic than the central North Atlantic because both oceans are open to the storms of the southern ocean (Webb, 1998), but to date there is little data from either basin. The infragravity-wave climate is known to be very low in the Arctic ocean in winter (Webb and Schultz, 1992), but otherwise we expect most sites on the seafloor will experience energetic infragravity waves and significant long-period noise due to wave loading.

Observations of Deformation under Infragravity Waves

Infragravity waves are evident in both seafloor pressure and acceleration records at frequencies below 0.04 Hz from a site SW of San Diego (31°24.765'N 118° 41.299'W; Fig. 1). The infragravity-wave noise completely obscures the pressure signal from a M_s 6.0 earthquake in the Aleutian Islands (51.6°N, 173.2°W, 14 September 1998, 23:16:46.8 GMT) and significantly raises vertical-acceleration noise levels. The vertical-acceleration measurements shown here are made with an autonomous, deep-ocean long-period seismometer system based on a Lacoste-Romberg gravimeter sensor (Crawford *et al.*, 1999). The pressure observations are made by one or more differential pressure gauges (DPG) on each instrument. In a DPG, a sensor measures the differ-

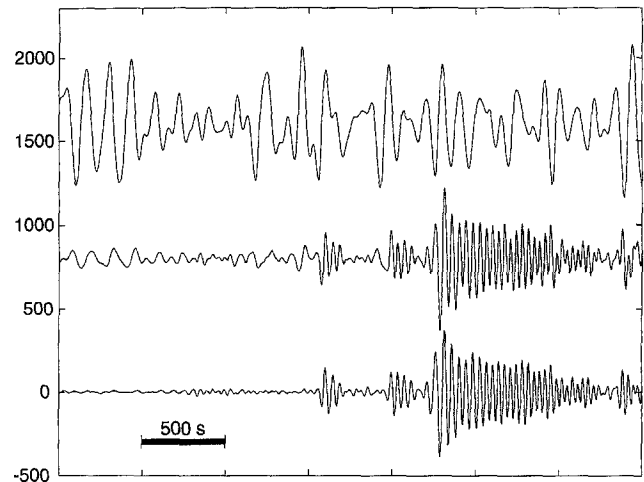


Figure 1. Top trace, differential pressure record filtered in the band from 0.008 to 0.04 Hz from a M_s 6.0 event in the Aleutian Islands observed at a site offshore of San Diego in 750 m of water. The infragravity waves completely obscure the event in the pressure record. Middle trace, filtered record of vertical acceleration from the same event. The deformation signal from infragravity waves is apparent before the body-wave arrivals. Bottom trace, the result of predicting the deformation signal from the pressure record and subtracting it from the acceleration record. The SNR for long-period phases has been improved by nearly 25 dB.

ence in pressure between the exterior of the gauge and a reference established within an oil-filled rigid container. Oil flow through a capillary leak allows the pressure in the reference to equilibrate with the ocean pressure on long time scales (Cox *et al.*, 1984). The technique allows very small pressure fluctuations to be detected in the presence of enormous ocean floor pressures.

The records in Figure 1 have not been corrected for instrument response. Corrected records would show the infragravity wave pressure and vertical acceleration signals in phase (displacement 180° out of phase) consistent with deformation under wave loading.

The pressure signal from any ocean wave decays approximately exponentially with depth below the sea surface with an e-folding distance equal to the wavenumber ($p = p_0/\cosh(kh)$). Short period ocean waves are too short in wavelength to produce significant pressure signals at the seabed. The observed pressure spectrum drops precipitously at frequencies above a corner frequency, which is a function of the water depth. The corner frequency for a depth of 750 m is about 0.03 Hz (Fig. 2a). The vertical acceleration also dips above this frequency, although other noise sources become important above 0.05 Hz (Fig. 2b). Above 0.1 Hz, both the pressure and acceleration spectra are dominated by microseisms, which are propagating seismic waves derived from ocean waves by other nonlinear processes (Webb, 1998).

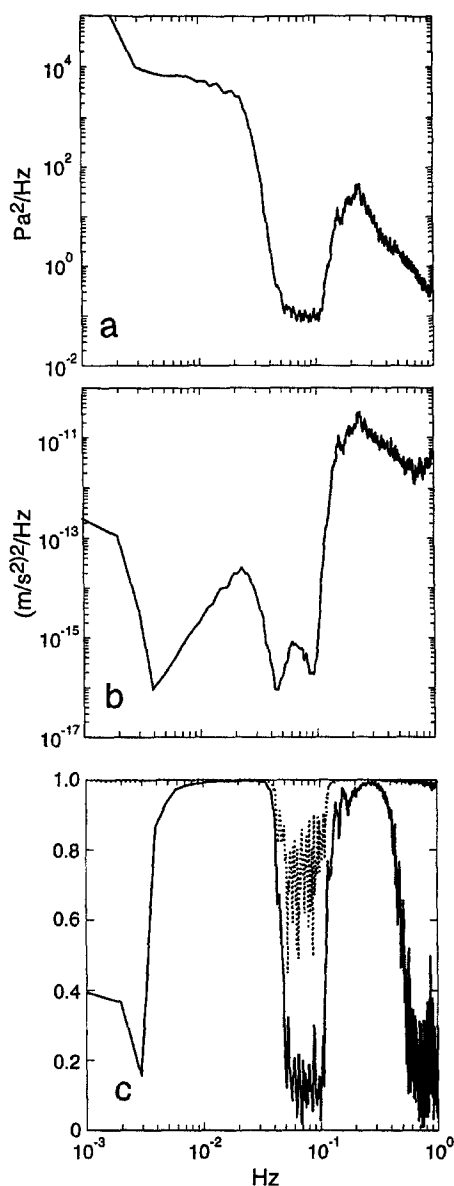


Figure 2. (a) The pressure seafloor pressure spectrum observed SW of San Diego. The infragravity-wave signal is clear at frequencies below 0.03 Hz. The microseism peak above 0.1 Hz is created by propagating elastic waves. (b) The acceleration spectrum at the same site. The deformation signal due to infragravity waves causes the peak in the spectrum between 0.002 and 0.025 Hz. The microseism peak is seen above 0.1 Hz. (c) Solid line, coherence between pressure and vertical acceleration; dashed line, coherence between two differential pressure gauges on the same instrument.

The coherence between pressure and vertical acceleration records is high in the infragravity-wave band from 0.003 to 0.04 Hz (Fig. 2c) demonstrating that in the absence of signals from large earthquakes, the long-period motion of the seafloor is controlled almost entirely by ground deformation under ocean-wave loading. The signals are incoher-

ent below 0.003 Hz because the deformation signal becomes too small to be detected above the seismometer noise level. Seismometer noise below 0.03 Hz may be due to current-induced tilt noise rotated into the vertical component because the vertical component is not perfectly aligned with the true vertical. The coherence is again high between 0.1 and 0.7 Hz in the microseism peak, but falls at frequencies above 0.7 Hz because the relationship between pressure and acceleration depends on more than one mode (Webb, 1992).

The transfer function between pressure and vertical acceleration was calculated from records of pressure and acceleration from the experiment (see following section). The transfer function increases with increasing frequency in the infragravity-wave band from 0.003 to 0.04 Hz (Fig. 3), which reflects the relatively larger deformation seen under shorter period waves. In the microseism peak, the acceleration is related to pressure by a complicated combination of the eigenfunctions of the relevant Rayleigh modes (Webb, 1992). The pressure signal due to infragravity waves is always relatively much larger than the acceleration signal, and seismic events will always be better detected by seismometers than by pressure measurements in the infragravity-wave band. At frequencies above the infragravity wave band, detection thresholds for seismic phases at the seafloor from pressure observations are similar to acceleration records (Webb, 1998).

Calculations of Transfer Functions and Seafloor and Subseafloor Deformation

The transfer function between pressure and vertical acceleration in the infragravity-wave band can be predicted from the elastic structure of the crust and upper mantle under a seafloor site and from the water depth above the site. This article focuses on using measurements of the transfer function combined with pressure records to remove the deformation signal from vertical seismic records. It should also be possible to use a transfer function calculated from direct knowledge of the elastic structure for this purpose, but because it is always necessary to record both pressure and acceleration, direct measurement of the transfer function is the more straightforward technique.

The dependence of the transfer function on crustal structure makes it also possible to use these measurements to study the oceanic crust. Techniques to calculate the transfer function from models of elastic structure have been developed in conjunction with studies of ridge crest magma bodies (Crawford *et al.*, 1998, 1999). The method works for mapping regions of melt within the oceanic crust because the seafloor undergoes relatively larger deformations at sites where the seafloor is underlain by regions of low-shear strength. In these regions, there are peaks in the transfer function which shift in frequency with changes in the depths to magma bodies.

The transfer function at a frequency f is the ratio of the acceleration $A(f)$ associated with an infragravity wave to the

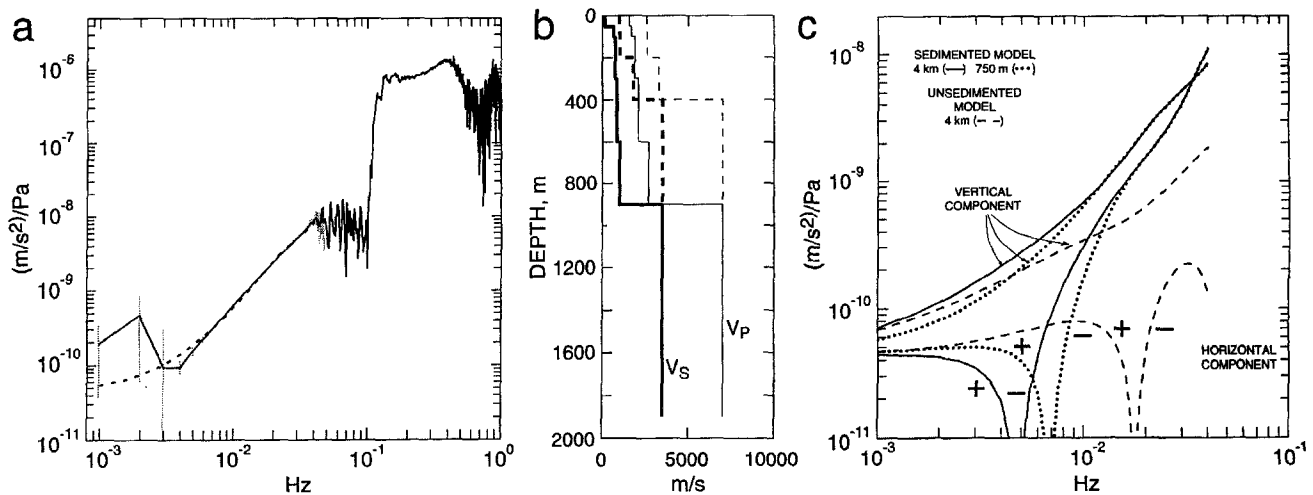


Figure 3. (a) Solid line, transfer function between pressure and vertical acceleration. 90% error bars are shown as vertical lines for frequencies below 0.05 Hz. The dashed line shows the transfer function calculated for the model shown in 3b. (b) Solid lines, a model of shear and compressional velocity for the experiment site; dashed lines, a model for an un-sedimented site. (c) Transfer functions between pressure and the vertical and horizontal acceleration for the models shown in (b) for water depths of 750 m or 4 km. The horizontal-transfer function changes sign, and positive and negative parts are labeled.

pressure signal $P(f)$ at the seafloor. The apparent acceleration due to infragravity waves is not entirely due to deformation; the variation in gravitational attraction associated with added mass under the wave crests and missing mass under the wave troughs produces an apparent acceleration. These gravitational accelerations become important at a long period (Crawford *et al.*, 1998; but note equation 6 has an extra factor of 2π). The apparent gravitational acceleration A' can be written in terms of the wave height h ; $A' \approx 2\pi G\rho h \exp(-kH)$, where G is the gravitational constant ($6.6732 \times 10^{-11} \text{ N m}^2 \text{ kg}^{-2}$), k is the wavenumber, ρ is the water density, and H is the vertical distance from the sea surface to the measurement point. Horizontal-component transfer functions can be calculated in a model that assumes the infragravity waves propagate in a single direction (both vertical and horizontal components are shown in Figure 3). The details of the calculations can be found in Crawford *et al.* (1998). The horizontal and vertical gravitational terms are equal in amplitude, but the horizontal gravitational and deformation terms are 90° out of phase with pressure and with vertical acceleration. The transfer functions shown in Figure 3 are controlled by the gravitational term below about 0.005 Hz.

The theoretical transfer functions depend on water depth through the dispersion relationship for the infragravity waves. Waves travel faster in deeper water, hence the wavelength of an infragravity wave increases with water depth. The transfer function at a particular frequency is affected by the elastic-wave velocities below the seafloor to depths comparable to about 1/6 of the infragravity-wave wavelength (Crawford *et al.*, 1991). The deformation is less under

regions with higher elastic velocities. The transfer function at lower frequencies depends on elastic structure to greater depths than higher frequencies because wavelengths are larger. The lowest frequency infragravity waves of interest here (0.005 Hz) are 17-km long, so the elastic structure of the top 3 km of crust is relevant to deformation calculations.

At most seafloor sites, elastic-wave velocities increase with depth below the seafloor, so the transfer functions increase monotonically with frequency. An elastic-wave model fitting the measured vertical transfer function (Fig. 3a) is consistent with a 1-km-thick layer of sediments overlying an igneous basement (Fig. 3b). The model is not strongly constrained by the data but appears to be geologically reasonable.

We show sets of transfer functions for two models of oceanic crust under 4 km of ocean, one with a deep sediment layer, the other without sediment (Fig. 3c). We also show results for the sedimented model under 750 m of ocean. The transfer function between pressure and horizontal acceleration is more complicated than the vertical-component transfer function and changes sign at a frequency that is dependent on the elastic structure and water depth (Fig. 3c). The model ignores the wave field directionality; if it were possible to obtain measurements of horizontal-transfer functions, the relative amplitude of the two horizontal components would depend on the directional spectrum of the infragravity-wave field. The directional spectrum of infragravity waves is often quite broad, if not isotropic, except near coastlines where bathymetric steering produces a narrower directional spectrum (Webb, 1986; Webb *et al.*, 1991; Herbers *et al.*, 1995).

The horizontal-component transfer function has yet to be measured on the deep seafloor because horizontal components tend to be dominated by tilt noise. Subtle tilts driven by ocean currents can raise noise levels at the seafloor by as much as 60 dB at a 100 sec period. It may be possible to measure the horizontal-component transfer functions using sensors buried beneath the seafloor or in boreholes. The next section shows it is possible to predict and suppress the vertical-component deformation signal using pressure measurements. Correcting for the horizontal-component deformation signal would be much more difficult because it requires array measurements of pressure fluctuations to establish the directional spectrum of infragravity-wave propagation.

The transfer functions between pressure and acceleration are only weakly dependent on water depth. The vertical-transfer function in 4 km-deep water is slightly larger at long period than the transfer function in a depth of 750 m, primarily because the phase velocity is larger in deep water (Fig. 3c). At higher frequencies, the phase velocity and the transfer functions are independent of water depth. Accelerations are larger on sedimented sites compared to hard rock (un-sedimented) sites. A difference of a factor of three in the near-surface shear modulus between two models (Fig. 3b) results in a similar difference in the transfer function (Fig. 3c) and results in 10 dB lower energy in the vertical-acceleration spectrum at short period at a hard rock site compared to a sedimented site (Fig. 4). Our two models have similar elastic structure at depth and predict similar seafloor acceleration spectra at low frequency.

The vertical acceleration spectrum has been estimated from the transfer-function calculation for two different water depths (Fig. 4), assuming the pressure spectrum from Figure 2a. Deformation noise is a bigger problem for seismology in shallow water because pressure fluctuations from shorter period waves can reach the seafloor. Near coastlines, the infragravity-wave pressure spectrum may also be higher due to topographic trapping, so seismic observations may be still noisier. Vertical component deformation noise in the Pacific is usually large enough to greatly limit observations of Rayleigh and long-period body waves at shallow seafloor sites. The vertical-component noise floor at good continental sites in the band from 0.0005 to 0.3 Hz is near 1×10^{-18} $(\text{m/s}^2)^2/\text{Hz}$ (Agnew *et al.*, 1978), while noise levels usually exceed 1×10^{-15} $(\text{m/s}^2)^2/\text{Hz}$ at deep sites on the Pacific seafloor and 1×10^{-14} $(\text{m/s}^2)^2/\text{Hz}$ at shallow sites. The infragravity-wave spectrum can be much less energetic in the North Atlantic. Beauduin and Montagner (1996) report values near 1×10^{-17} $(\text{m/s}^2)^2/\text{Hz}$ from the central North Atlantic, but noise levels this low are probably rare except during summer.

The deformation signal due to wave loading extends far below the seafloor because of the long wavelengths associated with infragravity waves (Fig. 4). The e-folding scale of decay with depth of the acceleration signal is approximately the inverse wavenumber of the ocean waves, although the acceleration signal also decreases with depth because of the

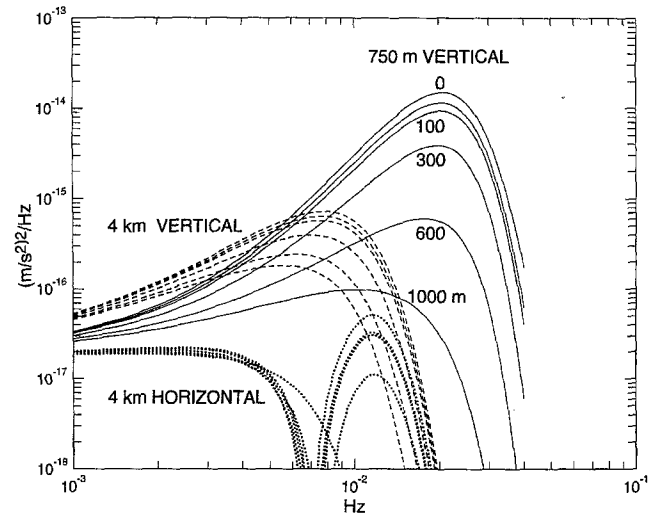


Figure 4. Predicted vertical-component-acceleration spectra for the sedimented model for a sensor at the seafloor (0 m) and at the depths shown below the seafloor in water depths of 750 m, solid lines, and 4 km, dash lines. Dotted lines, the seafloor horizontal-component-acceleration spectrum for a water depth of 4 km.

increasing elastic strength of the ground. Models of the vertical acceleration versus depth show that it will be necessary to place a seismometer more than 1000 m below the seafloor to obtain a 20 dB reduction in the deformation noise at 0.01 Hz. The signal decays more rapidly at higher frequency, but the decay at longer period is negligible, even at 1-km depth. The predicted horizontal acceleration spectrum is always significantly lower than the vertical acceleration spectrum (Fig. 4). Horizontal component deformation noise will only be a significant problem for sites in shallow water at short period. The horizontal- and vertical-acceleration transfer functions with pressure are approximately equal at short period (Fig. 3a).

Removing the Deformation Signal from the Vertical Component

Deformation noise will limit the signal-to-noise ratio for long-period seismic-phase observations, both for seafloor and buried seismometers, particularly in water depths less than 1 km. Measurements of seafloor pressure fluctuations can be used to predict the infragravity-wave-induced deformation so that this noise can be removed from vertical acceleration records. This process can greatly enhance the signal-to-noise ratio for long period phases (Fig. 1), although subtracting the deformation noise will slightly perturb the seismic observations because the pressure observations always include a small component associated with seismic phases. If necessary, this perturbation can be calculated and incorporated into modeling of Rayleigh-wave or body-wave synthetic seismograms.

One method to remove the deformation signal is in the Fourier domain. In the infragravity-wave band, the transfer function describes the vertical acceleration associated with the infragravity wave pressure signal as a function of frequency. The transfer function is first calculated from records of pressure and vertical acceleration, which have been selected to avoid instrument noise and seismic events. This transfer function should be applicable to all data sets from a site, since the transfer function should be only a function of the structure under the site and hence stationary in time. The transfer function $T(f)$ is bandpass filtered with a filter $W(f)$ centered on the infragravity-wave band so that only the deformation signal is included in the analysis. The Fourier transform of the predicted deformation signal for any record of acceleration is then $A'(f) = T(f) W(f) P(f)$ where $P(f)$ is the Fourier transform of the corresponding pressure record. $A'(f)$ is then subtracted from the Fourier transform of the acceleration record $A(f)$. The final step is calculating the inverse transform, obtaining an acceleration record with the deformation signal removed.

The previously mentioned method is not a particularly convenient way to correct the acceleration record. It is more convenient to work in the time domain. We start with a measurement of the transfer function between vertical acceleration and pressure derived from Fourier analysis of data sections free of obvious contamination from seismic events or instrumental noise. The ability to correct for the deformation signal will depend on how accurately the transfer function can be measured. The accuracy depends on the coherence between the acceleration and pressure signals and the length of the record. A longer record provides more degrees of freedom in estimating the transfer function, yielding a more accurate estimate. The coherence depends on noise sources in the pressure and acceleration records. It is important to select records without evidence of noise sources such as small earthquakes.

The next step is to construct a digital filter by applying an inverse Fourier transform to the transfer function after filtering the transfer function with a bandpass filter centered on the infragravity-wave band (for this example from 750 m water depth, the pass band is 0.003 to 0.05 Hz). The limits of the filter are not very important because the pressure signal falls sharply above 0.04 Hz, and the deformation signal is very small below 0.003 Hz. A digital filter constructed this way is shown in Figure 5. When convolved with the pressure record and subtracted from the vertical-acceleration record, it greatly reduces the infragravity wave signal on the vertical acceleration record (Fig. 1; bottom trace). The long period P -wave arrival is clearly visible early in the record, and spurious wiggles in the Rayleigh-wave train have been removed. This 25 dB reduction in noise level represents a huge improvement in detection threshold for long-period arrivals, and is equivalent to more than two units of earthquake magnitude in detection threshold (see Webb, 1998).

The actual improvement in noise level can be determined by comparing the vertical-acceleration spectrum from

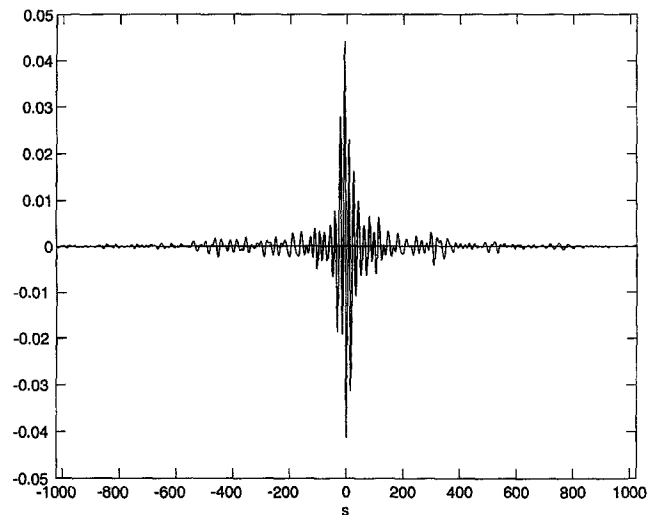


Figure 5. Digital filter calculated from the measured transfer function between pressure and vertical acceleration filtered between 0.006 and 0.1 Hz.

a quiet section of data, before and after correcting for the deformation signal (Fig. 6a). The noise reduction exceeds 25 dB between 0.01 Hz and 0.03 Hz (Fig. 6b). The vertical acceleration spectral level is flattened to near 1×10^{-16} (m/sec²)²/Hz in the infragravity-wave band (Fig. 6b). This reduction in noise level in the infragravity-wave band is very close to the maximum achievable reduction in noise level predicted from $1 - \gamma^2$, where γ is the coherence (Fig. 6b). The filter in this example was applied to a different section of data than was used to calculate the filter.

It is not easy to determine what establishes the noise floor for these observations. Lab tests show the instrumental noise floor for this seismometer is below the noise levels seen in Figure 6a. The coherence between pressure observations from two DPGs deployed on the instrument exceeds 0.995 across the entire infragravity-wave band, suggesting that noise in the pressure observations is also not the limiting factor (Fig. 2c).

Observations from deep water sites where the deformation signal is smaller can exhibit coherences between pressure and vertical acceleration exceeding 0.98 in the infragravity-wave band (see Crawford *et al.*, 1999), suggesting a factor of 15 dB improvement in vertical-component noise levels should be possible at these sites. This would push the effective vertical component noise floor to near 3×10^{-17} (m/sec²)²/Hz at those deep water sites.

Various possibilities limiting the coherence between pressure and vertical acceleration include the following: (1) the pressure signal may include a small component associated with forced rather than freely propagating ocean waves (Crawford, 1991). This component will be of smaller wavelength than the usual free wave infragravity wave signal and have a different transfer function, adding noise to the measured transfer function. (2) The transfer function may depend on the propagation direction of the infragravity waves

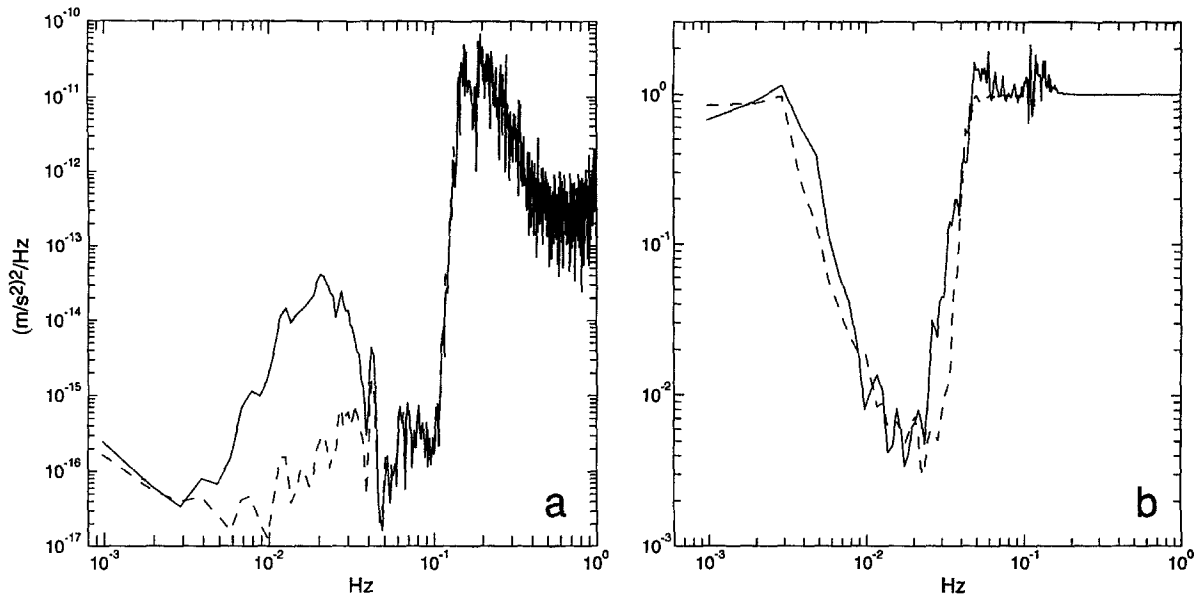


Figure 6. (a) Vertical-component-acceleration spectrum of data before (solid) and after (dashed line) removing the deformation signal calculated by convolving the pressure record with the digital filter. (b) Fractional reduction in spectral level obtained by removing the deformation signal (solid line). Theoretical limit for noise reduction inferred from $(1 - \gamma^2)$ where γ is the coherence (dashed line).

either because of bathymetry affecting the phase speed of the waves or because of variations in structure, particularly lateral variations in sedimentation. (3) Current-induced seismometer tilting could raise noise levels, although this source would likely show a frequency dependence with higher noise levels at longer period. Tracking down possible sources of noise will require further investigation.

Conclusions

Noise induced by deformation under the loading of long-period ocean waves (infragravity waves) limits the signal-to-noise ratio for long-period seismic phases for seismometers at or beneath the seafloor at most sites in the world's oceans. Borehole installation to depths of several hundred meters provides significant improvement in the signal-to-noise ratio only at the shorter periods. The deformation noise level depends on the amplitude of the ocean waves inducing the signal and on the elastic-wave velocities in the oceanic crust beneath a site. The deformation signal is larger on sedimented sites than on hard rock sites.

Pressure measurements of infragravity-wave amplitudes can be combined with measurements of the transfer function between pressure and vertical acceleration to predict and remove the deformation signal from seismic records. The deformation signal is most readily removed by constructing a digital filter from the transfer function, which is then convolved with the pressure record. Subtracting the predicted deformation signal from a vertical-acceleration record reduced noise levels by 25 dB in the band from 0.01 to 0.03

Hz in data from a site at a 750 m water depth near San Diego. Vertical-component spectral levels near 0.01 Hz were reduced from near 2×10^{-14} (m/sec²)²/Hz to below 1×10^{-16} (m/sec²)²/Hz, but remained above the noise levels seen at good continental sites [2×10^{-18} (m/sec²)²/Hz at 0.01 Hz; Agnew and Berger, 1978]. The horizontal component of deformation should be less than 5×10^{-17} (m/sec²)²/Hz at deep water sites, but may be comparable to the vertical component at frequencies above 0.02 Hz at sites in shallow water (<1 km depth).

Any installation of long-period seismometers on the seafloor should include one or more differential pressure gauges or other means of measuring pressure fluctuations in the frequency band from 0.001 to 0.04 Hz. The pressure measurements can be used to remove the noise signal due to deformation under wave loading, which leads to large improvements in the signal-to-noise ratio for observations of long-period phases.

Acknowledgments

This work was supported by the Office of Naval Research (N00014-96-1-0297). We would like to thank Randy Jacobson for a thorough review of the manuscript. Jacques Lemire and Tom Deaton were the principal engineers on the project.

References

- Agnew, D. C., and J. Berger (1978). Vertical seismic noise at very low frequencies, *J. Geophys. Res.* **83**, 5420–5424.
- Agnew, D. C. (1995). Ocean-load tides at the South Pole: a validation of recent ocean-tide models, *Geophys. Res. Lett.* **22**(22), 3063–3066.

- Beauduin, R., and J. P. Montagner (1996). Time evolution of broad-band seismic noise during the French pilot experiment OFM/SISOBS, *Geophys. Res. Lett.* **23(21)**, 2995–2998.
- Chave, A. D., F. K. Duennebie, R. Butler, R. A. Pettitt Jr., F. B. Wooding, A. D. Bowen, D. Harris, and D. R. Yoerger (1998). H20: the Hawaii-2 observatory, *EOS, Trans. Amer. Geophys. Soc.* **79(45)**, 65.
- Cox, C. S., T. Deaton, and S. C. Webb (1984). A deep sea differential pressure gauge, *J. Atm. Oceanic Tech.* **1(3)**, 237–246.
- Crawford, W. C., S. C. Webb, and J. A. Hildebrand (1991). Seafloor compliance observed by long period pressure and displacement measurements, *J. Geophys. Res.* **96**, 16151–16160.
- Crawford, W. C., S. C. Webb, and J. A. Hildebrand (1998). Estimating shear velocities in the oceanic crust from compliance measurements by two-dimensional finite-difference modeling, *J. Geophys. Res.* **103**, 9895–9916.
- Crawford, W. C., S. C. Webb, and J. A. Hildebrand (1999). Constraints on melt in the lower crust and Moho at the East Pacific Rise, 9°48'N, using seafloor compliance, *J. Geophys. Res.* **104(B2)**, 2923–2939.
- Farrell, W. E. (1972). Deformation of the Earth under surface loads, *Rev Geophys. Space Phys.* **10**, 761–797.
- Haubrich, R. A. (1970). The origin and characteristics of microseisms at frequencies below 140 cycles per hour, *IUGG Monogr.* **62**, 1753–1760.
- Herbers, T. H. C., S. Elgar, and R. T. Guza (1995). Generation and propagation of infragravity waves, *J. Geophys. Res.* **100**, 24863–24872.
- Lambert, A. (1970). The response of the Earth to loading by the ocean tides around Nova Scotia, *Geophys. J.R. Astro. Soc.* **19**, 449–477.
- Okiihiro, M., R. T. Guza, and R. J. Seymour (1992). Bound infragravity waves, *J. Geophys. Res.* **97**, 11453–11469.
- Webb, S. C., (1986). Coherent pressure fluctuations observed at two sites on the deep sea floor, *Geophys. Res. Lett.* **13(1)**, 141–144.
- Webb, S. C., X. Zhang, and W. C. Crawford (1991). Infragravity waves in the deep ocean, *J. Geophys. Res.* **96**, 2723–2736.
- Webb, S. C., and A. D. Schultz (1992). Very low frequency ambient noise at the seafloor under the Beaufort sea icecap, *J. Acoust. Soc. Amer.* **91(3)**, 1429–1439.
- Webb, S. C. (1992). The equilibrium oceanic microseism spectrum, *J. Acoust. Soc. Amer.* **94(4)**, 2141–2158.
- Webb, S. C. (1998). Broad seismology and noise under the ocean, *Rev. of Geophysics* **36**, 105–142.

Scripps Institution of Oceanography,
University of California, San Diego,
La Jolla, CA 92093.
(S.C.W., W.C.C.)

Manuscript received 15 April 1999.